DELIVERABLE D6.3

# Control system for mini-grid use case

***PUBLIC***

M. F. Shehzad, M. B. Abdelghany,
V. Mariani, D. Liuzza, L. Glielmo (UniSannio)
*Quality Assurance: F. Zenith (SINTEF)*

| | |
|---|---|
| **Project acronym:** | HAEOLUS |
| **Project title:** | Hydrogen-Aeolic Energy with Optimised eLectrolysers Upstream of Substation |
| **Project number:** | 779469 |
| **Call:** | H2020-JTI-FCH-2017-1 |
| **Topic:** | FCH-02-4-2017 |
| **Document date:** | February 4, 2020 |
| **Due date:** | December 31, 2019 |
| **Keywords:** | Energy storage systems, hydrogen conversion, power to gas, energy management, model predictive control, mixed logic dynamics |

**Abstract:** The current deliverable explains the formulation of a multi level Model Predictive Control (MPC) policy for a wind-hydrogen plant in mini-grid use cases within the EU-FCH 2 JU (European Union Fuel Cells and Hydrogen 2 Joint Undertaking) funded project HAEOLUS.

In mini-grid use cases hydrogen production is required in order to store temporary surpluses of energy from renewables and to provide a demand-side management solution for energy supply, both in islanded mode and in connected mode with strong limitations in the export capacity.

This goal is achieved through a multi-level Model-Predictive Control with optimal load demand tracking and electricity market participation. In order to capture both continuous/discrete dynamics and switching be tween different operating conditions, the plant is modeled according to the mixed logic dynamic framework.

## Revision History

| Date | Description | Author (organisation) |
|---|---|---|
| 2019/November/18 | First draft | Muhammad Faisal Shehzad (UniSannio) |
| 2019/December/2 | Add Abstract, Introduction | Muhammad Faisal Shehzad (UniSannio) |
| 2019/December/9 | Add System modeling | Muhammad Faisal Shehzad (UniSannio) |
| 2019/December/12 | Controller design | Muhammad Faisal Shehzad (UniSannio) |
| 2019/December/22 | Controller design | Muhammad Faisal Shehzad (UniSannio) |
| 2019/December/24 | Introduction | Muhammad Faisal Shehzad (UniSannio) |
| 2019/December/27 | Controller design | Muhammad Faisal Shehzad (UniSannio) |
| 2019/December/30 | Revision | Valerio Mariani (UniSannio) |
| 2019/January/08 | System modeling | Muhammad Faisal Shehzad (UniSannio) |
| 2019/January/13 | Revision | Valerio Mariani (UniSannio) |
| 2019/January/21 | Mini-grid connected mode controller design | Muhammad Faisal Shehzad (UniSannio) |
| 2019/January/23 | Revision | Valerio Mariani (UniSannio) |
| 2019/January/25 | Revisions addressed | Muhammad Faisal Shehzad (UniSannio) |
| 2019/January/27 | Review text for issues and inconsistencies fixing | Valerio Mariani (UniSannio) |
| 2019/January/30 | Revisions addressed | Muhammad Faisal Shehzad (UniSannio) |
| 2019/February/3 | Review text for issues and inconsistencies fixing | Valerio Mariani (UniSannio) |
| 2019/February/4 | Revisions addressed | Muhammad Faisal Shehzad (UniSannio) |

*This project has received funding from the Fuel Cells and Hydrogen 2 Joint Undertaking under the European Union's Horizon 2020 research and innovation programme under grant agreement № 779469.*

## Table of Contents

# 1 Introduction

In deliverables D6.1 and D6.2 the dynamic models for the HAEOLUS wind-hydrogen system and the control algorithm for the energy-storage use case have been presented, respectively. In the energy-storage use case the hydrogen production is meant to achieve power smoothing, mitigating the short-term fluctuations in power production by wind generation and thus facilitating wind power integration at large scales. In addition, in D6.2 the proposed controller also minimizes the operational costs, the maintenance costs and the degradation of the electrolyzer and the fuel cell.

The present deliverable develops the control system for mini-grid use cases where "*The main purpose of hydrogen production is the storage of temporary surpluses of energy from renewables and the provision of a demand side management solution for energy supply (the electrolyser serving as a controllable/dispatchable load)*" [1].

In mini-grid use cases two scenarios have to be considered, the first one corresponding to islanded mini-grids and the second one corresponding to (weakly)connected mini-grids with strong export limitations. Both fit with the actual conditions of the wind-farm operated by Varanger Kraft where the link with the main grid enables up to 95MW of export capacity.

The proposed controller will suit both the islanded and the connected modes by taking into account for different related aspects. In islanded mode the electrolyzer and the fuel cell will be operated in order to meet the load demand as required. In turn, the load demand tracking is achieved at two different time-scales, that are handled by the proposed algorithm. For the scenario under investigation, a larger time-scale involves load demand tracking with 1 hour sampling time while a shorter time-scale, that will be referred by the term real-time, involves load demand tracking with 1 minute sampling time. As a consequence, a two level controller architecture is proposed, each level dealing with strategies to be implemented in one corresponding time-scale. We agree the higher level controller provide actuation policies fitting the largest time-scale while the lower level controller provide actuation policies fitting the shortest time-scale. Also, the minimization of the operational costs, the maintenance costs and the degradation of the electrolyzer and the fuel cell will be included as in D6.2.

In connected mode, the additional participation to the electricity market will be also managed. The electricity market is a complex process of auctions where participants (sellers and buyers) propose, before gate closure, their quantity-price bids over the following delivery period. In case the bids are day-ahead, the market is usually referred as spot market. However, since participants are financially responsible for any deviation from the contract [2], certain electricity pools also integrate intraday markets, where it is possible to take corrective actions [3]. Since the load is still present and its forecasted demands have to be met, in connected mode a very wide and complex variety of possible operating strategies for the electrolyzer and the fuel cell may be achieved. In principle also in this case, two different time-scales have to be managed by the controller. However, since for the project scenario no real-time market is actually available, the low-level controller just implement on the shorter time-scale what scheduled by the high-level controller. This also allows us to consistently keep the previously mentioned two level architecture across the two different modes (islanded and connected).

The load demand tracking of a hydrogen based ESS is developed, solved, and experimentally validated under a complete 24-h test for both intraday and real time energy markets by using sample times of $T_s$ = 1 hour and $T_s$ = 1 min, respectively.

## 2 Nomenclature

The parameters, the forecasts and the decision variables used in the proposed formulation are described, respectively, in Tables 1–4.

Table 1: Parameters.

| Parameters | Description |
|---|---|
| $H^{\max}$ | Maximum level of the hydrogen storage unit [kg] |
| $H^{\min}$ | Minimum level of the hydrogen storage unit [kg] |
| $P_e^{\max}$ | Maximum power level of the electrolyzer [kW] |
| $P_e^{\min}$ | Minimum power level of the electrolyzer [kW] |
| $P_e^{\mathrm{STB}}$ | Standby power of the electrolyzer [kW] |
| $P_e^{\mathrm{CLD}}$ | Standby power of the electrolyzer [kW] |
| $P_e^{\mathrm{WRM}}$ | Standby power of the electrolyzer [kW] |
| $P_f^{\max}$ | Maximum power level of the fuel cell [kW] |
| $P_f^{\min}$ | Minimum power level of the fuel cell [kW] |
| $P_f^{\mathrm{STB}}$ | Standby power of the fuel cell [kW] |
| $P_e^{\mathrm{CLD}}$ | Standby power of the fuel cell [kW] |
| $P_e^{\mathrm{WRM}}$ | Standby power of the fuel cell [kW] |
| $\mathrm{NH}_e$ | Number of life hours of the electrolyzer [h] |
| $\mathrm{NH}_f$ | Number of life hours of the fuel cell [h] |
| $\mathrm{HY}_e$ | Number of per year life hours of the electrolyzer [h] |
| $\mathrm{HY}_f$ | Number of per year life hours of the fuel cell [h] |
| $S_{\mathrm{rep,i}}$ | Electrolyzer/Fuel cell stack replacement cost [€/kW] |
| $R_e$ | Ramp limit of the electrolyzer [kW/s] |
| $R_f$ | Ramp limit of the fuel cell [kW/s] |
| $\eta_e$ | Electrolyzer consumption [kg/Wh] |
| $\eta_f$ | Fuel cell consumption [Wh/kg] |
| $T$ | Simulation horizon [h] |
| $\Gamma$ | Energy price [€] |

## 3 System Description

The main components of the system under investigation are the wind generation unit, the hydrogen based storage system (electrolyzer, hydrogen tank and a fuel cell), the local loads, the

Table 2: Forecast powers.

| Forecasts | Description |
|---|---|
| $P_w$ | Wind power production [kW] |
| $P_{\mathrm{ref}}$ | Electrical load demand [kW] |

grid power and the control and communication systems. For sake of completeness a conceptual block diagram of the system is shown in Figure 1. The green solid lines denote energy flows, blue dashed lines show hydrogen flows and red dashed lines denote data flows. Accordingly, $P_w$ indicates the power generated by the wind farm, $P_{\mathrm{ez}}$ indicates the input power of the electrolyzer, $P_{\mathrm{fc}}$ indicates the output power of the fuel cell, $P_{\mathrm{grid}}$ is the grid exchanged power (sale or purchase), and $P_{\mathrm{ref}}$ is the reference demand which has to be tracked by $P_{\mathrm{avl}}$.

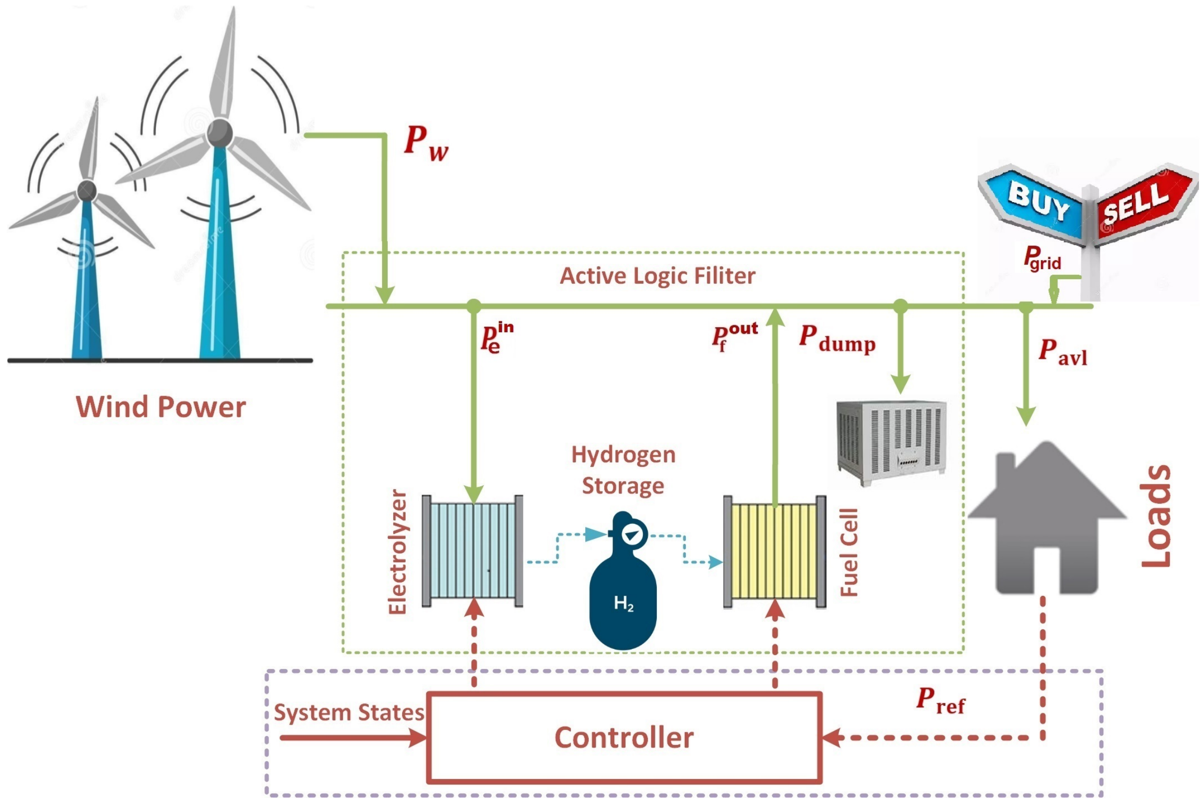


Figure 1: HAEOLUS' hydrogen based storage system modeled in this deliverable. $P_{\mathrm{e}}^{\mathrm{in}}$, $P_{\mathrm{f}}^{\mathrm{out}}$ and $P_{\mathrm{w}}$ are the electrolyzer input power, the fuel cell output power and the power achieved by wind generation, respectively. Also, $P_{\mathrm{ref}}$ is the reference demand and $P_{\mathrm{avl}}$ is the power available to downstream the plant.

Table 3: Real and logical time varying variables.

| Variables | Description |
|---|---|
| $\delta_e^{\mathrm{ON}}$ | On state of the electrolyzer |
| $\delta_e^{\mathrm{OFF}}$ | Off state of the electrolyzer |
| $\delta_e^{\mathrm{STB}}$ | Standby state of the electrolyzer |
| $\delta_f^{\mathrm{ON}}$ | On state of the fuel cell |
| $\delta_f^{\mathrm{OFF}}$ | Off state of the fuel cell |
| $\delta_f^{\mathrm{STB}}$ | Standby state of the fuel cell |
| $\delta_f^{\mathrm{CLD}}$ | Cold state of the fuel cell |
| $\delta_f^{\mathrm{WRM}}$ | Warm state of the fuel cell |
| $P_e$ | Electrical power of the electrolyzer [kW] |
| $P_f$ | Electrical power of the fuel cell [kW] |
| $P_{\mathrm{avl}}$ | Available system electrical power [kW] |
| $P_{\mathrm{dump}}$ | Dumped electrical power [kW] |
| $P_{\mathrm{grid}}$ | Grid power [kW] |
| $P_{\mathrm{grid}}^{\mathrm{sch}}$ | Scheduled grid power [kW] |
| $z$ | Electric power formulated as mixed logic dynamic (MLD) variables for the electrolyzer and the fuel cell [W] |
| $\sigma$ | Logical variables $\mathrm{ON/OFF/STB/CLD/WRM}$ states for the electrolyzer and the fuel cell |
| $\delta_{\mathrm{pch}}$ | Energy purchase logical variable |
| $\delta_{\mathrm{sale}}$ | Energy sale logical variable |
| $H$ | Stored level of hydrogen [kg] |

## 4 General Operations

The considered mini-grid use cases are divided into two general modes, grid-connected and islanded mode. The main difference between these operation modes is that in the grid-connected mode the purpose is to store surplus energy through storage units and provide demand response (DR) programs in a cost-optimized, environment friendly, and customer satisfying solution, and generally acting like the controllable load from the grid point of view. On the other hand, in islanded mode, the main purpose is maintaining the power balance between generation and demand without grid support.

More in details, in islanded mode, the load demand $P_{\mathrm{ref}}$ is met with the system available power $P_{\mathrm{avl}}$ only with no external exchange of energy sale or purchase i.e., in this mode $P_{\mathrm{grid}} = 0$. However, in connected mode, the plant is able to deliver power to the loads as well as able to exchange (sale or purchase) energy with the main grid based on the commitments made by

Table 4: Subscripts.

| Subscripts | Description |
|---|---|
| elz | Electrolyzer |
| fc | Fuel cell |
| grid | Main grid |
| pch | Purchase of energy |
| sale | Sale of energy |
| IM | Intraday energy market |
| R | Real time energy market |
| con | Connected mode |
| isl | islanded mode |
| HL | High level control |
| LL | Low level control |

the bidding in intraday energy market. The global cost function

$$\begin{aligned} J^{\mathrm{HL}} &= J_{\mathrm{isl}}^{\mathrm{HL}} + J_{\mathrm{con}}^{\mathrm{IM}} \delta^{\mathrm{con}} \\ J^{\mathrm{LL}} &= J_{\mathrm{isl}}^{\mathrm{LL}} + J_{\mathrm{con}}^{\mathrm{R}} \delta^{\mathrm{con}}, \end{aligned} \tag{1}$$

is considered, where $J_{\mathrm{isl}}^{\mathrm{HL}}$ explains the high level control load tracking implementation based on the dynamic hydrogen plant model delivered in D6.1, $J_{\mathrm{isl}}^{\mathrm{LL}}$ has been presented in deliverable D6.2, whereas $J_{\mathrm{con}}^{\mathrm{IM}} \delta^{\mathrm{con}}$ and $J_{\mathrm{con}}^{\mathrm{R}} \delta^{\mathrm{con}}$ cover the grid support in both high and low level controls, respectively. It is important to highlight here that as per definition of the "Mini-grid use cases" defined by International Energy Agency [1], only the load tracking part of the deliverable D6.2 (neglecting the output power smoothing) has been considered in D6.3. The connected mode has given an extra business features to the wind farm owners to participate into the electricity bidding process in case they want to exchange (sale or purchase) energy with the main grid. Thus, $\delta^{\mathrm{con}}$=1 explains that both high and low level controls take into account the local loads as well as exchanges contracted power with the main grid. Conversely, $\delta^{\mathrm{con}}$=0 shows that the operator is not interested in exchanging power with the main grid, rather pushing system to keep delivering to the local loads with out the grid support.

We remind the reader that D6.3 is designed to solve two different energy markets, so this is important to highlight here that the superscripts $\mathrm{IM}$, $\mathrm{R}$, $\mathrm{HL}$, $\mathrm{LL}$ refers to intraday market, real time market, high level control and low level control, respectively. For the sake of simplicity in order to achieve a better readability, we will not use such superscripts unless in minor circumstances when ambiguities may arise.

# 5 Mini-grid Connected Mode Controller Design

The different time scales of the electricity markets make a whole control algorithm necessary solving the long-term horizon schedule made by the daily market (24 h ahead) and the real-time load sharing (few minutes) (more information about the electrical market can be found in [4]). The costs and constraints of the ESS based on the life and load cycling degradation, as well as the deviation schedule penalty are managed using a two-level-cascaded MPC controller. The block diagram of the two-level controller is shown in Figure 2. The horizon of each control level is dictated by the time scale of the corresponding market. In addition to the considered costs, the MPCs are tuned giving bigger weights to degradation costs of the fuel cell and the electrolyzer, since these devices are more sensitive to degradation.

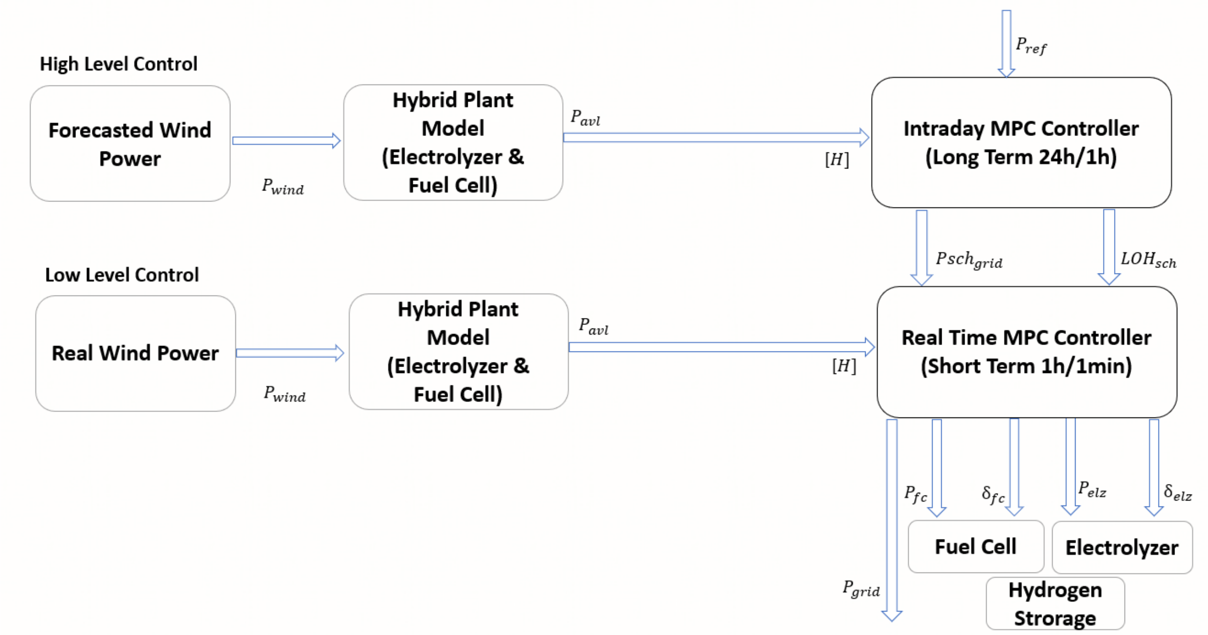


Figure 2: Multi-level Cascaded MPC Control Blockdiagram.

## 5.1 High Level Mathematical Modelling and Control

This section explains the modeling and the MPC control strategy to handle electricity transactions for the following day and to meet the load demand. The control goal is to find the optimal power schedule profiles for the electrolyser and the fuel cell so as to deliver power to the grid, to the load, to minimize operational costs and to maximize power sold revenues. We refer the reader to D6.1 for the details on the formulation of the mathematical models used by the high level controller and briefly reported in the following for sake of completeness.

### 5.1.1 Electrolyzer and Fuel Cell Models

The electrolyzer and the fuel cell have been both modeled as a three states automaton, as shown in Figure 3. For each one of them, the three states on $(\mathrm{ON})$, off $(\mathrm{OFF})$ and standby

$(\mathrm{STB})$ are considered. Correspondingly, the mutually exclusive logical variables $\delta_i^{\alpha}(k)$, with $\alpha \in \{\mathrm{OFF}, \mathrm{STB}, \mathrm{ON}\}$ and $i \in \{e, f\}$, are used to indicate the operating conditions of the electrolyzer ($i = e$) and the fuel cell ($i = f$) at any time $k$. More in detail, each operational

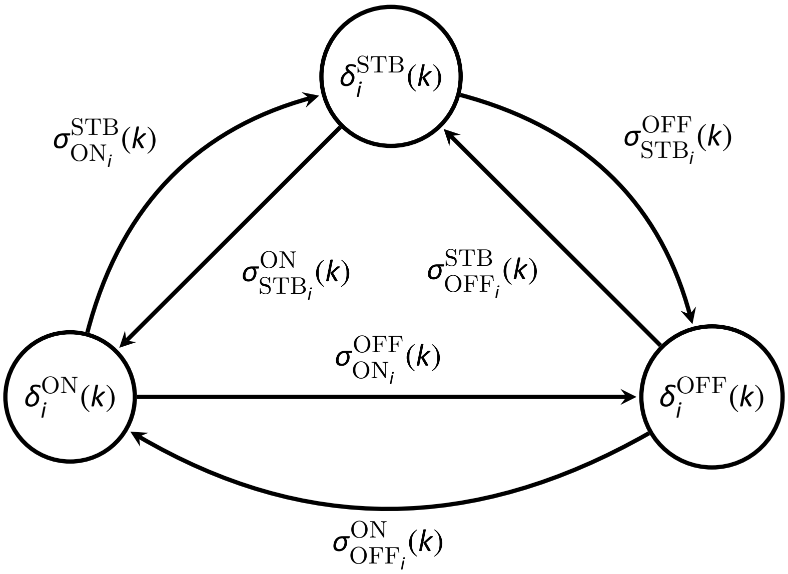


Figure 3: Automata of the electrolyzer ($i = e$) and of the fuel cell ($i = f$). Each node represents a particular state (i.e., operational mode), while the edges represent the state transition, for each $i \in \{e, f\}$.

state of the electrolyzer and the fuel cell results in a particular product of one logical variable and one corresponding power, which is relevant for that state, to be different from zero. For example, whenever the electrolyzer is in $\mathrm{ON}$ state, the corresponding input power is limited within the range $[P_e^{\mathrm{min}}, P_e^{\mathrm{max}}]$. Thus, by defining $P_e(k)\delta_e^{\mathrm{ON}}(k) = P_e^{\mathrm{in}}$ and since in this case we set $\delta_e^{\mathrm{ON}}(k) == 1$, which results $P_e(k) = P_e^{\mathrm{in}} \in [P_e^{\mathrm{min}}, P_e^{\mathrm{max}}]$. However, in standby state, the advantage of having warm start of the devices have been achieved with the tradeoff of delivering constant $1kW$ power to keep the devices stacks warm, and in this case $\delta_i^{\mathrm{STB}}(k) = 1$. Finally, when the electrolyzer is in $\mathrm{OFF}$ state, the input power along with the power consumption is null, resulting in $P_e(k) = 0$.

Along with the logical states, also the feasible state transitions among them have been modeled by means of the additional logical variables $\sigma_{\alpha_i}^{\beta}(k)$, with $\alpha \neq \beta$, $\beta \in \{\mathrm{OFF}, \mathrm{STB}, \mathrm{ON}\}$ and $i \in \{e, f\}$ and which can be defined by suitably combining the logical states through logical connectives. Both state variables and transition variables are codified with mixed integer linear inequalities which are included as constraints into the MPC controller. The mathematical formulation of these constraints is reported, for the reader convenience, in the Appendix A. We also refer the reader to deliverable D6.1 for proper understanding of all the formulated system operational constraints.

### 5.1.2 Hydrogen Storage Model

The relevant dynamics that will be used as constraints into the proposed controller are given by the changes in the Level of Hydrogen ($LoH$) in the tank. They depend on the reference power set points given to the electrolyzer and the fuel cell, but also on the operating state of the electrolyser and the fuel cell, that is

$$H(k+1) = H(k) + \eta_e P_e(k)\delta_e^{ON}(k)T_s - \frac{P_f(k)\delta_f^{ON}(k)T_s}{\eta_f}, \quad (2)$$

where $H(k)$ is the hydrogen level in the tank, while $\eta_e$ and $\eta_f$ are the hydrogen production and consumption rates of the electrolyzer and of the fuel cell, respectively. In general, the influence of the charge/discharge of the storage units on the stored energy levels is not the same, so different efficiencies for charge/discharge have been considered.

### 5.1.3 Power Balance Constraints

The power balance between energy production and consumption must be reached at each time $k$; hence the following equality constraints must hold

$$P_w(k) - P_e(k)\delta_e^{ON}(k) + P_f(k)\delta_f^{ON}(k) - P_{avl}(k) - P_{dump}(k) - P_{grid}(k) = 0. \quad (3)$$

The above equation contains also a term $P_{dump}$, which may be conveniently exploited (if a dumping load is available in the plant) to help the storage system in the power operations. $P_{grid}$ is the sale or purchase power commitment through participation in the intraday market. It can be clearly seen from the given formula that the system power $P_{avl}$ depends on the available wind power $P_w$, the balancing action of the hydrogen storage system and the dumping load (if present).

### 5.1.4 Physical and Operating Constraints

The system physical and operating constraints i.e., ramp up constraints, and hydrogen storage tank constraints have been taken into account in MPC control. We refer the reader to (D6.1, D6.2) for the detailed understanding on these constraints formulation.

### 5.1.5 MPC Design

The purpose of the intraday market is to handle electricity transactions for the following day through the presentation of electricity sale and purchase bids by market participants. Bids made by these sellers are presented to the market operator and will be included in a matching procedure that will affect the daily programming schedule corresponding to the following day. The outputs of the controllers are the reference power values for the ESS, for each hour of the day. The sample period used for this control level is $T_s$ = 1 h.

### 5.1.6 Global Cost Function

Taking into account the considerations in Sec. 4, the global cost function is considered

$$J_{con} = \sum_{j=1}^{T} \Big[\rho_{grid} J_{grid}(k+j) + \rho_i J_i(k+j) + \rho_l J_l(k+j)\Big] T_s, \quad (4)$$

where $J_{\mathrm{grid}}$, $J_i$, and $J_l$ are the grid, electrolyzer, fuel cell and load demand tracking cost functions, respectively, will be minimized, while $\rho_{\mathrm{grid}}$, $\rho_{\mathrm{i}}$ and $\rho_{\mathrm{l}}$ are the weighting factors used to achieve meaningful and dimensionless operation of the cost functions regardless of their unit measures. In the next subsections, (4) will be particularized for each cost function.

### 5.1.7 Grid Cost Function

The cost function that we propose in order to optimize the economic performance of the wind farm is

$$J_{grid}(k+J) = \Gamma_{\mathrm{pch}}(k+j)P_{\mathrm{pch}}(k+j), \tag{5}$$

where $T_s$ is the sampling time, $\Gamma_{\mathrm{pch}}$ is the energy price profile and $P_{\mathrm{pch}}$ is the power purchase from the grid through bidding. The minimization of (5) will results in purchasing the power when the prices are lower. Power sale and purchase with the grid are expressed by the introduction of two logical variables $\delta_{\mathrm{sale}}(k)$ and $\delta_{\mathrm{pch}}(k)$ which are active 1 or inactive 0, depending on the exchange of power with the main grid $P_{\mathrm{grid}}$.

These piecewise functions are introduced in the MPC controller using the transformation explained by Bemporad and Morari [5], resulting in the MLD constraints expressed in the inequalities (19)-(24). The detailed MLD formulation for the intraday market grid cost function has been done with the introduction of the logical and dynamic variables and is reported in the appendix A.

### 5.1.8 Operating Cost Function

The cost incurred in operating the electrolyzer and the fuel cell are summarized in the two respective cost functions derived in this section. Both are expressed as a summation of different costs related to the component depreciation, the reduction of life cycles and the energy spent in keeping the units warm during the stand by mode. This lifetime is expressed as a number of working hours. The lifetime can also be reduced if the degradation aspects related to this technology are not minimized. For this reason, not only the working hours for electrolyzer and fuel cells are minimized but the startup/shutdown/standby cycles and the fluctuations in the operation conditions are also included. It has been noticed in many studies [6, 7, 8, 9, 10] that the fluctuating loads and the operating cycles can seriously affect these devices in a number of ways. Therefore, in order to tackle such outlined problems, we propose the following cost, with $i \in \{e, f\}$

$$
\begin{aligned}
J_i(k+J) = & \left(\frac{S_{\mathrm{rep},i}}{\mathrm{NH}_i} + \mathrm{Cost}_i^{\mathrm{OM}}\right)\delta_i^{\mathrm{ON}}(k+j) \\
& + \mathrm{Cost}_{\mathrm{OFF}_i}^{\mathrm{ON}}\sigma_{\mathrm{OFF}_i}^{\mathrm{ON}}(k+j) \\
& + \mathrm{Cost}_{\mathrm{ON}_i}^{\mathrm{OFF}}\sigma_{\mathrm{ON}_i}^{\mathrm{OFF}}(k+j) \\
& + \mathrm{Cost}_{\mathrm{ON}_i}^{\mathrm{STB}}\sigma_{\mathrm{ON}_i}^{\mathrm{STB}}(k+j) \\
& + \mathrm{Cost}_{\mathrm{STB}_i}^{\mathrm{ON}}\sigma_{\mathrm{STB}_i}^{\mathrm{ON}}(k+j) \\
& + \mathrm{Cost}_{\mathrm{STB}_i}^{\mathrm{OFF}}\sigma_{\mathrm{STB}_i}^{\mathrm{OFF}}(k+j) \\
& + \mathrm{Cost}_{\mathrm{OFF}_i}^{\mathrm{STB}}\sigma_{\mathrm{OFF}_i}^{\mathrm{STB}}(k+j) \\
& + c(k)P_i^{\mathrm{STB}}\delta_i^{\mathrm{STB}}(k+j),
\end{aligned}
\tag{6}
$$

where $\mathrm{Cost}_e^{\mathrm{OM}}$ and $\mathrm{Cost}_f^{\mathrm{OM}}$ denote the operating and maintenance cost of the electrolyzer and the fuel cell, $c(k)$ is the power spot price, $\mathrm{NH}_e$ is the number of life hours of the electrolyzer and $\mathrm{NH}_f$ is the number of life hours of the fuel cell. $\mathrm{Cost}_{\mathrm{OFF}_i}^{\mathrm{ON}}$, $\mathrm{Cost}_{\mathrm{ON}_i}^{\mathrm{OFF}}$, $\mathrm{Cost}_{\mathrm{STB}_i}^{\mathrm{ON}}$, $\mathrm{Cost}_{\mathrm{ON}_i}^{\mathrm{STB}}$, $\mathrm{Cost}_{\mathrm{STB}_i}^{\mathrm{OFF}}$, and $\mathrm{Cost}_{\mathrm{OFF}_i}^{\mathrm{STB}}$ describe the startup, shutdown and standby cost of the electrolyzer and the fuel cell, respectively choosing $i \in \{e, f\}$. The $S_{\mathrm{rep},e}$ and $S_{\mathrm{rep},f}$ represent the stack replacement cost of the electrolyzer and the fuel cell, respectively.

#### 5.1.9 Load Tracking Cost Function

One goal of the system is to track the local load demand $P_{\mathrm{ref}}$ with the available system power $P_{\mathrm{avl}}$ in the best possible and economical way which we set to achieve by minimizing

$$
J_l(k+J) = \Big(P_{\mathrm{avl}}(k+j) - P_{\mathrm{ref}}(k+j)\Big)^2. \tag{7}
$$

## 5.2 Low Level Mathematical Modelling and Control

In Figure 2, the block diagram for the MPC controller is shown. The real time controller receives as a reference the energy and power reference scheduled by the intraday market MPC of the mini-grid for the electrolyzer, and the fuel cell, as well as the energy exchange with the main grid. The reason to introduce a double reference gives a freedom degree in the controller allowing to correct deficit scenario with exceeding scenario in comparison with the forecast carried out at the intraday market. While the high level controller has a control horizon of 24 h and a $T_s$ =1 hour, the real time MPC controller has a control horizon of 1 hour (a value taken due to the start sequence of the electrolyzer) and a $T_s$ =1 min. The use cascade control MPC allows us to manage from the long term control horizon given at the day-ahead MPC controller detailed in [4] linked to the real operational scenario object of this study. The purpose of the low level control is to track the references set by the high level control to match generation and load demands. The low level control will execute every 1 min and the control goals is to track the requested power in real time while minimizing the operational cost.

### 5.2.1 Electrolyzer and Fuel Cell Models

This section explains the electrolzer and the fuel cell models to solve real time energy market. As explained in the high level devices models, the electrolyzer and the fuel cell can be operated in 3 different physical modes, namely the on, the off and the stand-by mode. However, in low level control modelling, the short time features of both the devices have also been taken into account. The additional $\mathrm{CLD}$ and $\mathrm{WRM}$ states are included in order to account for cold and warm starts within the cost functions. As a consequence, the proposed controller will have to decide whether to switch off or put in stand-by the devices according to a trade-off between cold start, warm starts and operations in stand-by; the latter requiring a constant power from the grid even though their production/consumption is null [11].

Figure 4 shows the mode transitions that the electrolyzer and the fuel cell can undergo. It is important to highlight that those affecting the operating costs of the electrolyzer and the fuel cell are between the states $\mathrm{ON}$–$\mathrm{OFF}$, $\mathrm{CLD}$–$\mathrm{STB}$ and $\mathrm{STB}$–$\mathrm{OFF}$.

With considerations similar to those in Sec. 5.1.1, also in this case, electrolyzer and fuel cell

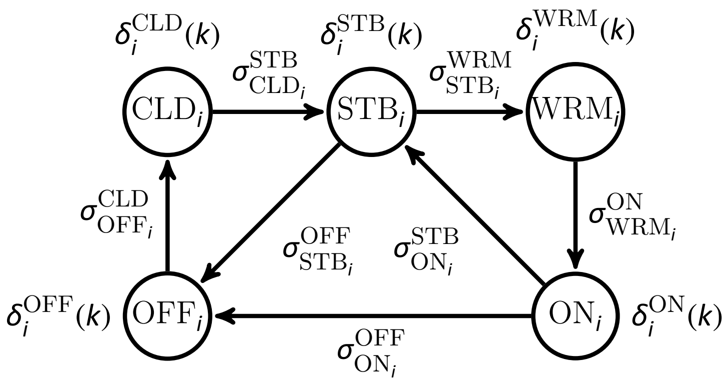


Figure 4: Five state automaton of the electrolyzer (i=e) and the fuel cell (i=f). The states $\mathrm{CLD}$ and $\mathrm{WRM}$ are used to take into account for the different switching times $T^{\mathrm{CLD}}$ and $T^{\mathrm{WRM}}$, of cold and warm starts, respectively, where typically $T^{\mathrm{CLD}} > T^{\mathrm{WRM}}$.

models depending on logical variables and state transitions are achieved. Then, they are codified with mixed integer linear inequalities which will be then included as constraints for the low level MPC controller. The mathematical formulation of these constraints is reported, for the reader convenience, in the Appendix B. We also refer the reader to deliverable D6.2 where the same approach with a similar scenario (warm and cold starts) has been also presented.

### 5.2.2 Hydrogen Storage Model

The hydrogen level dynamics for the low level controller are modeled with similar equations to those used for the high level controller, providing that now $\delta_e^{\mathrm{ON}}$, $\delta_f^{\mathrm{OFF}}$ refer to the five states automaton of the electrolyzer and the fuel cell, respectively, and $T_s = 1$ minute.

### 5.2.3 System Operating and Physical Constraints

The system operating and physical constraints i.e., power balancing equation, ramp up/down constraints have been modelled and formulated with similar equations used for high level control providing that all the relevant variables have to be referred to the low level and $T_s$ = 1 min.

### 5.2.4 MPC Design

The real time MPC controller helps to match generation and load within time ranges of order of minutes. There is a penalty deviation cost used as an incentive for the market participants to maintain their power balance. A consideration must be taken into account of the importance of the reference levels marked for the ESS in every hour by the previous MPC controllers. The low level MPC is executed every 1 minute with a scheduled horizon (SH) of 1 h discretized in periods of 60 minutes.

### 5.2.5 Global Cost Function

The cost function we purpose to optimize the optimal load sharing of the real scenario is

$$J_{\mathrm{con}}(k,m) = \sum_{p=1}^{SH} \Big[\rho_{\mathrm{grid}} J_{\mathrm{grid}}(k,m+p) + \rho_{\mathrm{i}} J_{\mathrm{i}}(k,m+p) + \rho_{\mathrm{l}} J_{l}(k,m+p)\Big] T_s, \tag{8}$$

where $\rho_{\mathrm{grid}}, \rho_{\mathrm{i}}$, and $\rho_{\mathrm{l}}$ are the weighting factors for dimensionless analysis of the low level control cost function. In the next subsections, (8) will be particularized for the ESS.

### 5.2.6 Grid Cost Function

Due to the high penalties imposed by the system operator in the real time market, the tracking deviation of the power exchange with the main grid $P_{\mathrm{grid}}$ versus the contracted-schedule with the Market/System Operator is considered. The cost function of the grid is

$$J_{\mathrm{grid}}(k,m+p) = \Gamma_{\mathrm{pch}}(k,SH)\Delta P_{\mathrm{pch}}(k,m+p), \tag{9}$$

where $\Gamma_{\mathrm{pch}}$ is the same price profile provided in the intraday market, because in Norwegian markets the prices are given on hourly basis, and $\Delta P_{\mathrm{pch}}(k,m+p)$ is the tracking deviation of power exchange with the grid and the contracted scheduled grid power. Power sale and purchase at real time energy market with the grid are expressed by the introduction of two logical variables $\delta_{\mathrm{pch}}(k,m)$ and $\delta_{\mathrm{sale}}(k,m)$. The detailed MLD formulation (33)-(37) for the real time market grid cost function has been done with the introduction of the logical and dynamic variables and is reported in the Appendix B.

### 5.2.7 Operating Cost Function

The economical dispatch of the microgrid gives both references the schedule in energy and in power at each instant. The operating cost of the use of hydrogen ESS for the real time market level control is a penalty from the final instant of the control horizon combined with the aspects of degradation and useful cost of this system with $i \in \{e, f\}$

$$
\begin{aligned}
J_{\mathrm{i}}(k, m+p) = & \left(\frac{S_{\mathrm{rep,i}}}{\mathrm{NH}_i} + \mathrm{Cost}_{\mathrm{i}}^{\mathrm{OM}}\right) \delta_{\mathrm{i}}^{\mathrm{ON}}(k, m+p) \\
& + \mathrm{Cost}_{\mathrm{ON_i}}^{\mathrm{OFF}} \sigma_{\mathrm{ON_i}}^{\mathrm{OFF}}(k, m+p) \\
& + \mathrm{Cost}_{\mathrm{CLD_i}}^{\mathrm{STB}} \sigma_{\mathrm{CLD_e}}^{\mathrm{STB}}(k, m+p) \\
& + \mathrm{Cost}_{\mathrm{STB_i}}^{\mathrm{OFF}} \sigma_{\mathrm{STB_i}}^{\mathrm{OFF}}(k, m+p) \\
& + c(k) P_{\mathrm{i}}^{\mathrm{STB}} \delta_{\mathrm{i}}^{\mathrm{STB}}(k, m+p) \\
& + c(k) P_{\mathrm{i}}^{\mathrm{CLD}} \delta_{\mathrm{i}}^{\mathrm{CLD}}(k, m+p) \\
& + c(k) P_{\mathrm{i}}^{\mathrm{WRM}} \delta_{\mathrm{i}}^{\mathrm{WRM}}(k, m+p) \\
& + \omega_{\mathrm{tank}}^{E} \left(H^{LL}(k, m+p) - H^{HL}(k, m+p)\right)^2 \\
& + \sum_{\alpha \in \mathscr{A}} \omega_{\mathrm{i}}^{P} \left(P_{\mathrm{i}}^{LL,\alpha}(k, SH) \delta_{\mathrm{i}}^{LL,\alpha}(k, SH) - P_{\mathrm{i}}^{HL,\alpha}(k) \delta_{\mathrm{i}}^{HL,\alpha}(k)\right)^2,
\end{aligned} \tag{10}
$$

where $\omega_{\mathrm{tank}}^{E}$ is the weighting factor for the deviation in energy stored in the hydrogen tank for lower level control with respect to the energy schedule given in the high level control, $\mathscr{A}$=$\{\mathrm{ON,COLD,STB,WRM,OFF}\}$ and $\omega_{\mathrm{i}}^{P}$ are the terms to penalize the power deviation of electrolyzer and the fuel from their high level control scheduled power. The weights $\omega_{\mathrm{tank}}^{E}$ and $\omega_{\mathrm{i}}^{P}$ have proper measurement units so to consistently achieve homogeneous terms in (10). The power spot price, the devices transitions and the costs related to them has been considered the same providing in the high level control devices operating cost functions.

### 5.2.8 Load Tracking Cost Function

For real-time operations, the load tracking is achieved through the minimization of

$$
J_l(k, m+p) = \left(P_{\mathrm{avl}}^{R}(k, SH) - P_{\mathrm{ref}}(k)\right)^2 + \lambda_{\epsilon} \epsilon, \tag{11}
$$

where $k \in \{1, \ldots, 24\}$ is the high level MPC index, while $\lambda$ is a penalty factor introduced to minimized the $\epsilon$ rapidly. Since there is not an energy forecast model the controller uses directly the real-time measurements (generation and consumptions) to calculate the real time market available power $P_{\mathrm{avl}}$. The controller assumes that these values are going to be constant during the prediction horizon. The double references (forecast and real time) gives a freedom degree in the controller to correct power deficit scenario with exceeding scenario, and in order to achieve this, equation (11) must be considered with the following additional constraint

$$
P_{\mathrm{avl}}^{R}(k, SH) - P_{\mathrm{avl}}^{\mathrm{IM}}(k) \leq \epsilon \tag{12}
$$

The cascaded control sequence allows us to link long term control horizon given at the day-ahead MPC controller to the real operational scenario.

# A Appendix A

## A.1 Intraday MPC Constraints Formulation of the Logical States

The meaning of $P_i(k)$ depends on the condition of the $i$-th device that, in turn, is identified by the corresponding $\delta_i^\alpha(k)$. That is, $P_i^\alpha = P_i\delta_i^\alpha(k)$, and therefore, according to the operating condition of the $i$-th device, each $\delta_i^\alpha(k)$ is determined as

$$\begin{cases} P_i^{\min} \le P_i(k) \le P_i^{\max} & \iff \delta_i^{\mathrm{ON}} = 1, \\ P_i(k) = P_i^{\mathrm{STB}} & \iff \delta_i^{\mathrm{STB}} = 1, \\ P_i(k) = 0 & \iff \delta_i^{\mathrm{OFF}} = 1. \end{cases} \tag{13}$$

In order to cope with an optimal control framework we need to introduce the auxiliary Boolean variables $z_i^\gamma(k) \in \{0,1\}$, with $\gamma \in \{\ge 0, \le 0, \ge P_i^{\mathrm{STB}}, \le P_i^{\mathrm{STB}}, \ge P_i^{\min}, \le P_i^{\max}\}$ and $i \in \{e,f\}$ [5]

$$z_i^{\gamma^{\ge}}(k) = \begin{cases} 1 & P_i(k) \ge \gamma, \\ 0 & P_i(k) < \gamma, \end{cases} \tag{14a}$$

$$z_i^{\gamma^{\le}}(k) = \begin{cases} 0 & P_i(k) > \bar{\gamma}, \\ 1 & P_i(k) \le \bar{\gamma}, \end{cases} \tag{14b}$$

with $(\gamma^{\ge}, \gamma^{\le}) \in \{(\ge 0, \le 0), (\ge P_i^{\mathrm{STB}}, \le P_i^{\mathrm{STB}}), (\ge P_i^{\min}, \le P_i^{\max})\}$ and $(\gamma, \bar{\gamma}) \in \{(0,0), (P_i^{\mathrm{STB}}, P_i^{\mathrm{STB}}), (P_i^{\min}, P_i^{\max})\}$. Then, (14) can be expressed as

$$\begin{aligned} P_i(k) - \gamma &< M z_i^{\gamma^{\ge}}(k), \\ -P_i(k) + \gamma &\le M\left(1 - z_i^{\gamma^{\ge}}(k)\right); \end{aligned} \tag{15a}$$

$$\begin{aligned} -P_i(k) + \bar{\gamma} &< M z_i^{\gamma^{\le}}(k), \\ P_i(k) - \bar{\gamma} &\le M\left(1 - z_i^{\gamma^{\le}}(k)\right); \end{aligned} \tag{15b}$$

where $M$ is a sufficiently large positive number.

The auxiliary variables codified by the inequalities (15) are then exploited to model the Mixed-Linear Dynamic (MLD) by linking the discrete logical variables of each device with the corresponding operating power. Namely, for $i \in \{e,f\}$, $\alpha \in \{\mathrm{OFF}, \mathrm{STB}, \mathrm{ON}\}$, the variables $\delta_i^\alpha(k) \in [0,1]$ are determined by

$$\left(1 - \delta_i^\alpha(k)\right) + z_i^{\gamma^{\ge}}(k) \ge 1, \tag{16a}$$

$$\left(1 - \delta_i^\alpha(k)\right) + z_i^{\gamma^{\le}}(k) \ge 1. \tag{16b}$$

Notice that, despite $\delta_i^\alpha(k)$ being continuous, they can only assume the binary values $\{0,1\}$ due to (16), that is in practice $\delta_i^\alpha(k)$s are logical.

## A.2 Intraday Market Mathematical Model and Constraints Formulation of the State Transitions

As discussed above, the devices models are characterized by three discrete operational states. These operational states imply possible mode transitions for each device. In what follows, we define all of the transitions. The transitions among the states for the each transition is the result of the state change, and can be defined by suitably combining logical variables, thus achieving

$$\sigma_{\alpha_i}^{\beta}(k) = \delta_i^{\alpha}(k-1) \wedge \delta_i^{\beta}(k), \tag{17}$$

with $\alpha$, $\beta \in \{\mathrm{OFF}, \mathrm{STB}, \mathrm{ON}\}$, $\alpha \neq \beta$. Using the relationships defined by Bemporad and Morari [5], each expression of the (17) is equivalently converted into three inequalities and introduced in the constraints of MPC controller, thus resulting in the 18 following formulas

$$\begin{aligned} -\delta_i^{\alpha}(k-1) + \sigma_{\alpha_i}^{\beta}(k) &\leq 0, \\ -\delta_i^{\beta}(k) + \sigma_{\alpha_i}^{\beta}(k) &\leq 0, \\ \delta_i^{\alpha}(k-1) + \delta_i^{\beta}(k) - \sigma_{\alpha_i}^{\beta}(k) &\leq 1. \end{aligned} \tag{18}$$

where $\sigma_{\alpha_i}^{\beta} \in [0, 1]$, and analogously to $\delta_i^{\alpha}(k)$s, they can only assume values $\{0, 1\}$ due to (18).

## A.3 Intraday Market Controller Grid MLD Formulation

The conversions introduced by Bemporad and Morari [5] make it possible to include binary and auxiliary variables introduced in a discrete-time dynamic system in order to describe, in a unified model, the evolution of the continuous and logic signals of the system. Thus,

$$\delta_{\mathrm{pch}}(k) = \begin{cases} 1, & P_{\mathrm{pch}}(k) = P_{\mathrm{grid}}(k), \\ 0, & P_{\mathrm{pch}}(k) = 0 \end{cases} \tag{19a}$$

$$\delta_{\mathrm{sale}}(k) = \begin{cases} 0, & P_{\mathrm{sale}}(k) = 0, \\ 1, & P_{\mathrm{sale}}(k) = P_{\mathrm{grid}}(k) \end{cases} \tag{19b}$$

where

$$P_{\mathrm{pch}}(k) = P_{\mathrm{grid}}(k)\delta_{\mathrm{pch}}(k) \tag{20}$$

$$P_{\mathrm{sale}}(k) = P_{\mathrm{grid}}(k)\delta_{\mathrm{sale}}(k) \tag{21}$$

$$P_{\mathrm{grid}}(k) = P_{\mathrm{pch}}(k) - P_{\mathrm{sale}}(k). \tag{22}$$

$$\begin{cases} P_{\mathrm{pch}}(k) \leq M_{\mathrm{pch}}\delta_{\mathrm{pch}}(k) \\ P_{\mathrm{pch}}(k) \geq m_{\mathrm{pch}}\delta_{\mathrm{pch}}(k) \\ P_{\mathrm{pch}}(k) \leq P_{\mathrm{grid}}(k) - m_{\mathrm{pch}}(1 - \delta_{\mathrm{pch}}(k)) \\ P_{\mathrm{pch}}(k) \geq P_{\mathrm{grid}}(k) - M_{\mathrm{pch}}(1 - \delta_{\mathrm{pch}}(k)) \end{cases} \tag{23a}$$

$$\begin{cases} P_{\text{sale}}(k) & \leq & M_{\text{sale}}\delta_{\text{sale}}(k) \\ P_{\text{sale}}(k) & \geq & m_{\text{sale}}\delta_{\text{sale}}(k) \\ P_{\text{sale}}(k) & \leq & P_{\text{grid}}(k) - m_{\text{sale}}(1-\delta_{\text{sale}}(k)) \\ P_{\text{sale}}(k) & \geq & P_{\text{grid}}(k) - M_{\text{sale}}(1-\delta_{\text{sale}}(k)) \end{cases} \tag{23b}$$

$$\delta_{\text{sale}}(k) + \delta_{\text{pch}}(k) \leq 1. \tag{24}$$

# B Appendix B

## B.1 Real Time MPC Constraints Formulation of the Logical States

According to the operating condition of the electrolyzer and of the fuel cell, each $\delta_i^\alpha(k)$ with $i \in \{e, f\}$ is determined at any time $k$ as follows

$$\begin{cases} P_i^{\min} \leq P_i(k) \leq P_i^{\max} & \iff \delta_i^{\text{ON}} = 1, \\ P_i(k) = P_i^{\text{CLD}} & \iff \delta_i^{\text{CLD}} = 1, \\ P_i(k) = P_i^{\text{STB}} & \iff \delta_i^{\text{STB}} = 1, \\ P_i(k) = P_i^{\text{WRM}} & \iff \delta_i^{\text{WRM}} = 1, \\ P_i(k) = 0 & \iff \delta_i^{\text{OFF}} = 1. \end{cases} \tag{25}$$

In order to cope with an optimal control framework, the cases in (25) need further manipulations to derive MILP constraints [5]. For this reason, as an intermediate step, we introduce auxiliary Boolean variables defined as

$$z_i^{\gamma^{\geq}}(k) = \begin{cases} 1 & P_i(k) \geq \gamma, \\ 0 & P_i(k) < \gamma, \end{cases} \tag{26a}$$

$$z_i^{\gamma^{\leq}}(k) = \begin{cases} 0 & P_i(k) > \bar{\gamma}, \\ 1 & P_i(k) \leq \bar{\gamma}, \end{cases} \tag{26b}$$

with $(\gamma^{\geq}, \gamma^{\leq}) \in \{(\geq 0, \leq 0), (\geq P_i^{\text{CLD}}, \leq P_i^{\text{CLD}}), (\geq P_i^{\text{STB}}, \leq P_i^{\text{STB}}), (\geq P_i^{\text{WRM}}, \leq P_i^{\text{WRM}}), (\geq P_i^{\min}, \leq P_i^{\max})\}$ and $(\gamma, \bar{\gamma}) \in \{(0,0), (P_i^{\text{CLD}}, P_i^{\text{CLD}}), (P_i^{\text{STB}}, P_i^{\text{STB}}), (P_i^{\text{WRM}}, P_i^{\text{WRM}}), (P_i^{\min}, P_i^{\max})\}$. By using the transformations defined in [5], the (26) can be expressed with the following compact inequalities for each cases:

$$\begin{aligned} P_i(k) - \gamma &< M z_i^{\gamma^{\geq}}(k), \\ -P_i(k) + \gamma &\leq M\left(1 - z_i^{\gamma^{\geq}}(k)\right); \end{aligned} \tag{27a}$$

$$\begin{aligned} -P_i(k) + \bar{\gamma} &< M z_i^{\gamma^{\leq}}(k), \\ P_i(k) - \bar{\gamma} &\leq M\left(1 - z_i^{\gamma^{\leq}}(k)\right); \end{aligned} \tag{27b}$$

where $M$ is a suitably large positive number. The auxiliary Boolean variables $z_i^\gamma(k)$s in (27) are then exploited to model the MLD by linking the discrete logical variables of each device with the corresponding operating power, according to (25). Namely, for $i \in \{\mathrm{e}, \mathrm{c}\}$, the logical variables $\delta_i^\alpha \in [0,\ 1]$, with $\alpha \in \{\mathrm{OFF}, \mathrm{CLD}, \mathrm{STB}, \mathrm{WRM}, \mathrm{ON}\}$, are defined by

$$\left(1 - \delta_i^\alpha(k)\right) + z_i^{\gamma^{\geq}}(k) \geq 1, \tag{28a}$$

$$\left(1 - \delta_i^\alpha(k)\right) + z_i^{\gamma^{\leq}}(k) \geq 1. \tag{28b}$$

Since all the states are discrete and the devices will work only in one and only one mode at any time $k$, the additional constraint

$$\delta_i^{\mathrm{OFF}}(k) + \delta_i^{\mathrm{CLD}}(k) + \delta_i^{\mathrm{STB}}(k) + \delta_i^{\mathrm{WRM}}(k) + \delta_i^{\mathrm{ON}}(k) = 1 \tag{29}$$

has to be considered for each $i \in \{e, f\}$.

## B.2 Real Time MPC Mathematical Model and Constraints Formulation of the State Transitions

As discussed above, each device is modeled by means of a corresponding five states automaton. These operational states imply twenty possible mode transitions:

$$\sigma_{\alpha_i}^{\beta}(k) = \delta_i^\alpha(k-1) \wedge \delta_i^\beta(k), \tag{30}$$

with $\sigma_{\alpha_i}^{\beta} \in [0, 1]$, $\alpha, \beta \in \{\mathrm{OFF}, \mathrm{CLD}, \mathrm{STB}, \mathrm{WRM}, \mathrm{ON}\}$ and $\alpha \neq \beta$. In order to cope with MILP constraints, each equation in (30) is converted into three corresponding inequalities, thus resulting in

$$\begin{aligned} -\delta_i^\alpha(k-1) + \sigma_{\alpha_i}^{\beta}(k) &\leq 0, \\ -\delta_i^\beta(k) + \sigma_{\alpha_i}^{\beta}(k) &\leq 0, \\ \delta_i^\alpha(k-1) + \delta_i^\beta(k) - \sigma_{\alpha_i}^{\beta}(k) &\leq 1. \end{aligned} \tag{31}$$

As discussed above in the modelling section, our system is constrained to evolve only the admissible transitions, namely the ones depicted in Fig.4. For some of them, i.e., $\sigma_{\mathrm{ON}_i}^{\mathrm{OFF}}(k)$, $\sigma_{\mathrm{CLD}_i}^{\mathrm{STB}}(k)$, and $\sigma_{\mathrm{STD}_i}^{\mathrm{OFF}}(k)$ a cost is paid due to the stack degradation in switching from hydrogen production (or consumption) and not production (or consumption) and vice versa. These transitions have been explicitly modeled since they will appear in the devices cost functions. Furthermore, all the inadmissible transitions, i.e., all the ones other than those in Fig.4, have been defined and set to zero. It is important to highlight that, in order to force the evolution of the electrolyzer and the fuel cell modes according to each corresponding automaton as depicted in Fig. 4, for $i \in \{\mathrm{e}, \mathrm{f}\}$, in (31) all the transitions of the not appearing edges are set to zero, that is

$$\sigma_{\mathrm{OFF}_i}^{\mathrm{STB}}(k) = \sigma_{\mathrm{OFF}_i}^{\mathrm{WRM}}(k) = \sigma_{\mathrm{OFF}_i}^{\mathrm{ON}}(k) = 0, \tag{32a}$$

$$\sigma_{\mathrm{CLD}_i}^{\mathrm{OFF}}(k) = \sigma_{\mathrm{CLD}_i}^{\mathrm{WRM}}(k) = \sigma_{\mathrm{CLD}_i}^{\mathrm{ON}}(k) = 0, \tag{32b}$$

$$\sigma_{\mathrm{STB}_i}^{\mathrm{ON}}(k) = \sigma_{\mathrm{STB}_i}^{\mathrm{CLD}}(k) = 0, \tag{32c}$$

$$\sigma_{\mathrm{WRM}_i}^{\mathrm{OFF}}(k) = \sigma_{\mathrm{WRM}_i}^{\mathrm{CLD}}(k) = \sigma_{\mathrm{WRM}_i}^{\mathrm{STB}}(k) = 0, \tag{32d}$$

$$\sigma_{\mathrm{ON}_i}^{\mathrm{CLD}}(k) = \sigma_{\mathrm{ON}_i}^{\mathrm{WRM}}(k) = 0. \tag{32e}$$

## B.3 Low Level Controller Grid MLD Formulation

$$\delta_{\text{sale}}(k,m) = \begin{cases} 1, & (P_{\text{grid}}(k,m) - P^{\text{sch}}_{\text{grid}}(k)) \geq 0 \\ 0, & (P_{\text{grid}}(k,m) - P^{\text{sch}}_{\text{grid}}(k)) < 0 \end{cases} \tag{33a}$$

$$\delta_{\text{sale}}(k,m) = \begin{cases} 0, & (P_{\text{grid}}(k,m) - P^{\text{sch}}_{\text{grid}}(k)) \geq 0 \\ 1, & (P_{\text{grid}}(k,m) - P^{\text{sch}}_{\text{grid}}(k)) < 0. \end{cases} \tag{33b}$$

and

$$\Delta P_{\text{sale}}(k,m) = \left(P_{\text{grid}}(k,m) - P^{\text{sch}}_{\text{grid}}(k)\right).\delta_{\text{sale}}(k,m) \tag{34}$$

$$\Delta P_{\text{pch}}(k,m) = \left(P_{\text{grid}}(k,m) - P^{\text{sch}}_{\text{grid}}(k)\right).\delta^{\text{R}}_{\text{pch}}(k,m) \tag{35}$$

$$\begin{cases} \Delta P_{\text{sale}}(k,m) & \leq \; M_{\text{sale}}\delta_{\text{sale}}(k,m) \\ \Delta P_{\text{sale}}(k,m) & \geq \; m_{\text{sale}}\delta_{\text{sale}}(k,m) \\ \Delta P_{\text{sale}}(k,m) & \leq \; P_{\text{grid}}(k,m) - m_{\text{sale}}(1-\delta_{\text{sale}}(k,m)) \\ \Delta P_{\text{sale}}(k,m) & \geq \; P_{\text{grid}}(k,m) - M_{\text{sale}}(1-\delta_{\text{sale}}(k,m)) \end{cases} \tag{36a}$$

$$\begin{cases} \Delta P_{\text{pch}}(k,m) & \leq \; M_{\text{pch}}\delta_{\text{pch}}(k,m) \\ \Delta P_{\text{pch}}(k,m) & \geq \; m_{\text{pch}}\delta_{\text{pch}}(k,m) \\ \Delta P_{\text{pch}}(k,m) & \leq \; P_{\text{grid}}(k,m) - m_{\text{pch}}(1-\delta_{\text{pch}}(k,m)) \\ \Delta P_{\text{pch}}(k,m) & \geq \; P_{\text{grid}}(k,m) - M_{\text{pch}}(1-\delta_{\text{pch}}(k,m)) \end{cases} \tag{36b}$$

$$\delta_{\text{sale}}(k,m) + \delta_{\text{pch}}(k,m) \leq 1. \tag{37}$$

# References


[1] "Iea-hia task 24 wind energy & hydrogen integration," ieahydrogen.org › pdfs › Task_24_final_report.

[2] P. Pinson, C. Chevallier, and G. N. Kariniotakis, "Trading wind generation from short-term probabilistic forecasts of wind power," *IEEE Transactions on Power Systems*, vol. 22, no. 3, pp. 1148–1156, 2007.

[3] F. Morata and I. S. Sandoval, *European energy policy: An environmental approach*. Edward Elgar Publishing, 2012.

[4] F. Garcia-Torres, L. Valverde, and C. Bordons, "Optimal load sharing of hydrogen-based microgrids with hybrid storage using model-predictive control," *IEEE Transactions on Industrial Electronics*, vol. 63, no. 8, pp. 4919–4928, 2016.

[5] A. Bemporad and M. Morari, "Control of systems integrating logic, dynamics, and constraints," *Automatica*, vol. 35, no. 3, pp. 407–427, 1999.

[6] F. Alavi, E. P. Lee, N. van de Wouw, B. De Schutter, and Z. Lukszo, "Fuel cell cars in a microgrid for synergies between hydrogen and electricity networks," *Applied Energy*, vol. 192, pp. 296–304, 2017.

[7] M. Petrollese, L. Valverde, D. Cocco, G. Cau, and J. Guerra, "Real-time integration of optimal generation scheduling with MPC for the energy management of a renewable hydrogen-based microgrid," *Applied Energy*, vol. 166, pp. 96–106, 2016.

[8] M. Khalid and A. Savkin, "A model predictive control approach to the problem of wind power smoothing with controlled battery storage," *Renewable Energy*, vol. 35, no. 7, pp. 1520–1526, 2010.

[9] L. Olatomiwa, S. Mekhilef, M. Ismail, and M. Moghavvemi, "Energy management strategies in hybrid renewable energy systems: A review," *Renewable and Sustainable Energy Reviews*, vol. 62, pp. 821–835, 2016.

[10] A. Núñez-Reyes, D. M. Rodríguez, C. B. Alba, and M. Á. R. Carlini, "Optimal scheduling of grid-connected pv plants with energy storage for integration in the electricity market," *Solar Energy*, vol. 144, pp. 502–516, 2017.

[11] "Hydrogen-aeolic energy with optimized electrolysers upstream of substation project," http://www.haeolus.eu/.